Appl. Phys. B (2013) 112:193–201
DOI 10.1007/s00340-013-5417-2

Applied Physics B
Lasers and Optics

Ultrashort pulse propagation and nonlinear frequency conversion in superconducting and magnetic photonic crystal

C. H. Raymond Ooi · Choo Yong Lee

Received: 6 January 2013 / Accepted: 12 March 2013 / Published online: 1 April 2013

Abstract We study the propagation and second harmonic generation of ultrashort pulse in nonlinear photonic crystal using a combination of Fourier transform and transfer matrix method. The focus is on the reflected and transmitted output of fundamental pump pulse and second harmonic pulse in frequency and time domains, the temperature dependence of the reflection and transmission spectra where the superconducting transition frequency is close to the magnetic resonance. Interesting features include output pump and second harmonic pulses that can be strongly modulated with the transmitted pulses being delayed by slow light effect.

1 Introduction

Photonic crystal structures can control the propagation of electromagnetic wave [1] and play an important role in developing various optical devices [2]. The multiple reflections of electromagnetic wave at the layer interface in one-dimensional photonic crystal lead to forbidden (photonic bandgap) region where electromagnetic field is reflected and strongly damped (evanescent wave) within the structure [3, 4].

Second harmonic generation (SHG) is important for generating higher frequency waves [5]. Pulsed SHG in one -imensional photonic band gap material doped with $\chi^{(2)}$ medium has been demonstrated [6]. SHG in metal and antiferromagnetic thin film has also been studied [7, 8]. Zhou et al. [9] also investigated SHG from antiferromagnetic film embedded in one-dimensional photonic crystal. It is shown that strong SHG would occur near photonic band edge [10]. In silicon photonic, second- and third-order susceptibilities are used to convert wavelengths in optical communication [11]. In many cases, phased matching is an important factor contributing to SHG enhancement. There are various approaches to enhance SHG in photonic crystal. One method is by using periodically poled photonic crystal [5, 12, 13]. Other methods use defect or cavity quantum electrodynamic effect[14, 15], disorder structure [16], pumping of slow light [17, 18], controlling of pump beam intensity [19] and introduction of Bragg reflector mirrors [20] in which strong localization of fundamental field (FF) enhances coupling of waves in $\chi^{(2)}$ medium.

Normally semiconductor or dielectric materials are used. Superconductor has not been used in nonlinear photonic crystal. The presence of bandgap at low-frequency region and its tunability with temperature make superconductor an attractive material for engineering optothermal devices for pulses in the far infrared (FIR) region. The two-fluid model [21, 22] provides a convenient description for investigation of band structure in superconducting photonic crystal [23]. Recently, optical properties of superconductor-ferromagnetic bilayer structure [24] have been studied using the two-fluid model.

Nonlinear PC introduces strong dispersion for spectral broadening and strong nonlinearity which enables pulse shaping and light-control-light functionality. Recent work shows SHG in periodically poled lithium niobate waveguide driven by femtosecond laser pulses [25]. Besides, generation of ultrashort pulse in organic crystal has been demonstrated in the range of 10–30 THz [26]. Split ring resonator [27] and thin wire array [28] can be used to yield frequency-dependent magnetic permeability and permittivity. The feasibility of SHG in metamaterials has been demonstrated [29, 30].

C. H. R. Ooi (✉) · C. Y. Lee
Department of Physics, University of Malaya,
50603 Kuala Lumpur, Malaysia
e-mail: rooi@um.edu.my

Here, we explore pulsed SHG in bilayer photonic crystal composed of superconductor combined with magnetic resonance to form negative refractive index region [31, 32]. The input pump pulse propagates through the nonlinear photonic crystal (NPC) while generating/producing a SH pulse through nonlinear frequency conversion process (see Fig. 1). The nonlinear photonic crystal converts a small fraction of energy in the pump laser pulse into SH signal by frequency doubling, even in the absence of seed second harmonic. The energy of the SH pulse is supplied by the input pump pulse which is assumed to be sufficiently strong such that the effects of depletion/distortion on the SH process are negligible so that the pump pulse inside the NPC can be assumed to be the input pulse. Also, the SHG can be assumed to be small so that the effects of nonlinear process (the SH signal) on the propagation of the pump pulse can be neglected. The SH pulse exists only when the pump pulse is present. Therefore, the process involves propagation of the pump pulse and production of the SH signal through frequency conversion. We shall analyze transmission and reflection spectra of the FF and SH fields with respect to temperature and the output SH pulse in frequency and time domains and show that the dispersive magnetic-superconductor photonic crystal provides a method for generating short pulse in the infrared (IR) region.

2 Model and method

We use transfer matrix method (TMM) to model electromagnetic wave propagation [33], harmonic generation for arbitrary wavevector directions [34] of SHG [35, 36] in the nonlinear photonic crystal driven by a pump laser or a fundamental field (FF). We develop transfer matrix in frequency domain.

For arbitrarily short pulse the SVEA is not valid. In order to obtain solutions where dispersion is fully incorporated, we use the formal solution in frequency domain that satisfies the homogeneous wave equation $\{\frac{\partial^2}{\partial z^2}+\frac{n_j^2(\omega)\omega^2}{c^2}\}\Omega_j(z,\omega)\simeq 0$ for propagation through the jth layer in the photonic crystal, which is

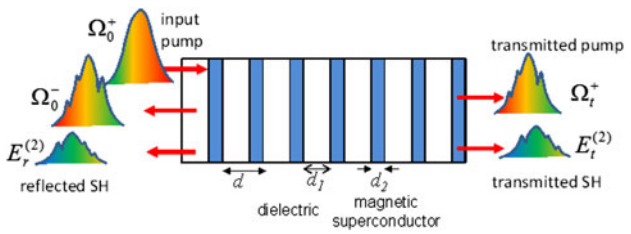

Fig. 1 An example of nonlinear photonic crystal with layer 1 and layer 2. One of the layers can be superconducting or/and magnetic. A pump pulse passes through and provides some of its energy to produce second harmonic pulse. The reflected and transmitted pump pulse and second harmonic pulse are shown

$$E_j(z,\omega)=\Omega_j^+(\omega)e^{ik_j(\omega)\left(z-z_{j-1}\right)}+\Omega_j^-(\omega)e^{-ik_j(\omega)\left(z-z_{j-1}\right)} \tag{1}$$

subjected to initial input pulse $\Omega_0^+(\omega)=\Omega_0^+\exp[-\left(\frac{\omega-\omega_L}{\sigma_L}\right)^2]$ with carrier frequency ω_L and bandwidth σ_L.

The linear propagation of layer j is governed by the refractive index

$$n_j(\omega)=\sqrt{\mu_j(\omega)\varepsilon_j(\omega)} \tag{2}$$

where μ_j and ε_j are frequency-dependent (dimensionless) relative permeability and permittivity of the medium induced by magnetic response and electric response. By using Maxwell equation $\nabla\times\mathbf{E}_j^{(1)}(z,\omega)=i\omega\mu_0\mu_j(\omega)\mathbf{H}_j(z,\omega)$, we have the magnetic field (along x-axis)

$$H_j^{(1)}(z,\omega)=\frac{\xi_j(\omega)}{c\mu_0}\left[\Omega_j^+(\omega)e^{ik_j(\omega)\left(z-z_{j-1}\right)}-\Omega_j^-(\omega)e^{-ik_j(\omega)\left(z-z_{j-1}\right)}\right] \tag{3}$$

where $\xi_j(\omega)=\frac{n_j(\omega)}{\mu_j(\omega)}$

We arrange Eqs. (1) and (3) in matrix form:

$$\begin{bmatrix} E_j^{(1)} & (z,\omega) \\ c\mu_0 H_j^{(1)} & (z,\omega)\end{bmatrix}=D_j\begin{bmatrix}\Omega_j^+(z,\omega)\\ \Omega_j^-(z,\omega)\end{bmatrix} \tag{4}$$

where $D_j=\begin{bmatrix}1 & 1\\ \xi_j(\omega) & -\xi_j(\omega)\end{bmatrix}$ is the matrix that describes the refractive index of individual layer.

Consider continuity of $E_j^{(1)}(z,\omega)$ and $H_j^{(1)}(z,\omega)$ and Maxwell boundary condition at interface of odd and even layers and input and output interface (air left and right of photonic crystal), we could obtain transfer matrix of FF wave propagation for N period

$$\begin{bmatrix}\Omega_t^+\\ 0\end{bmatrix}=\mathcal{T}^{(1)}\begin{bmatrix}\Omega_0^+\\ \Omega_0^-\end{bmatrix} \tag{5}$$

where $\mathcal{T}^{(1)}=D_0^{-1}L^N D_0=\begin{bmatrix}T_{11}^{(1)} & T_{12}^{(1)}\\ T_{21}^{(1)} & T_{22}^{(1)}\end{bmatrix}$ is the final transfer matrix, $D_0=\begin{bmatrix}1 & 1\\ n_0(\omega) & -n_0(\omega)\end{bmatrix}$, $n_0(\omega)$ is the refractive index of the air. The transfer matrix of single period is

$$L=D_2P_2D_2^{-1}D_1P_1D_1^{-1}. \tag{6}$$

Here, the propagation matrix that model the phase change is $P_j=\begin{bmatrix}e^{ik_j(\omega)d_j} & 0\\ 0 & e^{-ik_j(\omega)d_j}\end{bmatrix}$ with the layer thickness $z_j-z_{j-1}=d_j$. To facilitate precision computation, we have expressed $D_jP_jD_j^{-1}=\begin{bmatrix}\cos\theta_j & i\frac{\sin\theta_j}{x_j}\\ ix_j\sin\theta_j & \cos\theta_j\end{bmatrix}$ where $x_j=\frac{n_j^{(1)}}{\mu_j^{(1)}}$ and $\theta_j=k_j(\omega)d_j$ and obtained an analytical matrix for L.

The fields in the odd layers are

$$\begin{bmatrix} \Omega_{2j-1}^{+} \\ \Omega_{2j-1}^{-} \end{bmatrix} = D_1^{-1} L^{j-1} D_0 \begin{bmatrix} \Omega_0^{+} \\ \Omega_0^{-} \end{bmatrix} \tag{7}$$

and in the even layers

$$\begin{bmatrix} \Omega_{2j}^{+} \\ \Omega_{2j}^{-} \end{bmatrix} = D_2^{-1} D_1 P_1 D_1^{-1} L^{j-1} D_0 \begin{bmatrix} \Omega_0^{+} \\ \Omega_0^{-} \end{bmatrix}. \tag{8}$$

Equations (7) and (8) are used to compute the propagation of SH fields. The transmission and reflection coefficients are

$$t^{(1)} = \frac{\Omega_t^{+}}{\Omega_0^{+}} = \mathcal{T}_{11}^{(1)} - \mathcal{T}_{12}^{(1)} \frac{\mathcal{T}_{21}^{(1)}}{\mathcal{T}_{22}^{(1)}}, \quad r^{(1)} = \frac{\Omega_0^{-}}{\Omega_0^{+}} = -\frac{\mathcal{T}_{21}^{(1)}}{\mathcal{T}_{22}^{(1)}} \tag{9}$$

where, here, $\Omega_r^{(1)} = \Omega_0^{-}$ and $\Omega_t^{(1)} = \Omega_{2N}^{+}$. Hence, we determine the transmission $T^{(1)} = |t^{(1)}|^2$ and the reflection $R^{(1)} = |r^{(1)}|^2$ spectra.

Assuming a nonlinearly generated field in the jth layer is a plane wave which has no radial dependence, the vector wave equation $(\nabla^2 + \varepsilon_r \mu_j \frac{\omega^2}{c^2}) E_j = -\mu_o \mu_j \omega^2 P_j^{NL}$ in Fourier frequency domain ω becomes

$$\left(\frac{\partial^2}{\partial z^2} + k_j^2(\omega')\right) E_j^{(2)}(z,\omega') = -\mu_0 \mu_j(\omega') \omega'^2 P_j^{NL}(z,\omega') \tag{10}$$

where $k_j(\omega') = n_j(\omega')\frac{\omega'}{c}$ is the SH wavevector in the j-th layer. For SHG, the nonlinear polarization is

$$\begin{aligned} P_j^{NL}(z,\omega') &= \varepsilon_0 \chi_j^{(2)}(\omega') E_j^{(1)}(z,\omega)^2 \\ &= \varepsilon_0 \chi_j^{(2)}(2\omega) \Big[\left(\Omega_j^{+}(\omega)\right)^2 e^{i2k_j(\omega)\left(z-z_{j-1}\right)} \\ &\quad + \left(\Omega_j^{-}(\omega)\right)^2 e^{-i2k_j(\omega)\left(z-z_{j-1}\right)} + 2\Omega_j^{+}(\omega)\Omega_j^{-}(\omega) \Big] \end{aligned} \tag{11}$$

where $\omega' = 2\omega$.

Using Laplace transform to solve Eq. (10), we have the general solution of the SH field as

$$E_j^{(2)}(z,\omega') = \begin{bmatrix} E_j^{(2)+}(\omega) e^{ik_j(\omega')\left(z-z_{j-1}\right)} + E_j^{(2)-}(\omega) e^{-ik_j(\omega')\left(z-z_{j-1}\right)} \\ +A_j \left(\Omega_j^{+}(\omega)\right)^2 e^{i2k_j(\omega)\left(z-z_{j-1}\right)} + A_j \left(\Omega_j^{-}(\omega)\right)^2 e^{-i2k_j(\omega)\left(z-z_{j-1}\right)} + C_j 2\Omega_j^{+}(\omega)\Omega_j^{-}(\omega) \end{bmatrix} \tag{12}$$

$$A_j(\omega) = -\left(\frac{\omega'}{c}\right)^2 \frac{\mu_j(\omega')\chi_j^{(2)}(\omega')}{k_j^2(\omega') - 4k_j^2(\omega)}, \tag{13}$$

$$C_j(\omega) = -\left(\frac{\omega'}{c}\right)^2 \frac{\mu_j(\omega')\chi_j^{(2)}(\omega')}{k_j^2(\omega')}. \tag{14}$$

The SH magnetic field obtained from the Maxwell equation is Arranging $E_j^{(2)}(z)$ and $H_j^{(2)}(z)$ fields in the matrix form, we have

$$c\mu_0 H_j^{(2)}(z,\omega') = \begin{bmatrix} \frac{n_j^{(2)}(\omega')}{\mu_j^{(2)}(\omega')} \left(E_j^{(2)+}(\omega) e^{ik_j(\omega')\left(z-z_{j-1}\right)} - E_j^{(2)-}(\omega) e^{-ik_j(\omega')\left(z-z_{j-1}\right)}\right) \\ + \frac{n_j^{(1)}(\omega)}{\mu_j^{(2)}(\omega')} A_j \left(\left(\Omega_j^{+}(\omega)\right)^2 e^{i2k_j(\omega)\left(z-z_{j-1}\right)} - \left(\Omega_j^{-}(\omega)\right)^2 e^{-i2k_j(\omega)\left(z-z_{j-1}\right)} \right) \end{bmatrix} \tag{15}$$

$$\begin{bmatrix} E_j^{(2)}(z,\omega') \\ c\mu_0 H_j^{(2)}(z,\omega') \end{bmatrix} = G_j \begin{bmatrix} E_j^{(2)+}(z,\omega') \\ E_j^{(2)-}(z,\omega') \end{bmatrix} + B_j \begin{bmatrix} A_j \left(\Omega_j^{+}(z,\omega)\right)^2 \\ A_j \left(\Omega_j^{-}(z,\omega)\right)^2 \end{bmatrix} + 2C_j \begin{bmatrix} 1 \\ 0 \end{bmatrix} \Omega_j^{+}(z,\omega)\Omega_j^{-}(z,\omega) \tag{16}$$

For simplification, we define $E_j^{(2)\pm}(z,\omega') = E_j^{(2)\pm}(\omega)e^{\pm ik_j(\omega')}(z-z_{j-1})$ and $\Omega_j^{\pm}(z,\omega) = \Omega_j^{\pm}(\omega)e^{\pm ik_j(\omega)(z-z_{j-1})}$.

Again, we consider the continuity of $E_j^{(1)}(z,\omega)$ and $H_j^{(1)}(z,\omega)$ or the Maxwell boundary condition at the interface of odd and even layers, and input and output interfaces (air left and right ends of photonic crystal). Employing the transfer matrix of FF wave propagation for N period, we compute SH output (forward $E_t^{(2)+}$and backward $E_0^{(2)-}$) for $j = N > 0$

$$G_0\begin{bmatrix}E_t^{(2)+}(\omega)\\0\end{bmatrix} = S^N G_0\begin{bmatrix}E_0^{(2)+}(\omega)\\E_0^{(2)-}(\omega)\end{bmatrix} + \sum_{j=1}^{N} S^{N-j}\left[N_2M_1\vec{I}_{2j-1}(z) + M_2\vec{I}_{2j}(z) + N_2\vec{J}_1\Omega_{2j-1}^{+}(\omega)\Omega_{2j-1}^{-}(\omega) + \vec{J}_2\Omega_{2j}^{+}(\omega)\Omega_{2j}^{-}(\omega)\right] \tag{17}$$

where $S = N_2N_1$, $N_j = G_jQ_jG_j^{-1}(j=1,2)$, $M_j = A_j(B_jF_j - N_jB_j)$ and $\vec{J}_j = 2C_j[I - N_j]\vec{J}$. The matrices are defined as follows: $Q_j = \begin{bmatrix}e^{ik_j^{(2)}d_j} & 0\\0 & e^{-ik_j^{(2)}d_j}\end{bmatrix}$, $F_j = P_j^2 = \begin{bmatrix}e^{i2k_j(\omega)d_j} & 0\\0 & e^{-i2k_j(\omega)d_j}\end{bmatrix}$, $\vec{I}_\alpha(z) = \begin{bmatrix}\left(\Omega_\alpha^{+}(z)\right)^2\\\left(\Omega_\alpha^{-}(z)\right)^2\end{bmatrix}$ $(\alpha = 2j-1, 2j)$ and $\vec{J} = \begin{bmatrix}1\\0\end{bmatrix}$.

To prevent accumulated numerical errors, we use the matrix relation below [37] to find Nth power of any unimodular M matrix to compute S^N, S^{N-j} and L^N

$$M^N = \begin{bmatrix}m_{11}U_{N-1} - U_{N-2} & m_{12}U_{N-1}\\m_{21}U_{N-1} & m_{22}U_{N-1} - U_{N-2}\end{bmatrix} \tag{18}$$

where $U_N(a) = \frac{\sin\left[(N+1)\cos^{-1}a\right]}{\sqrt{1-a^2}}$ and $a = \frac{1}{2}(m_{11}+m_{22})$.

For convenience, we define $D_m = G_0^{-1}S^NG_0 = \begin{pmatrix}D_{11}^{(2)} & D_{12}^{(2)}\\D_{21}^{(2)} & D_{22}^{(2)}\end{pmatrix}$ and the second term on RHS of Eq. (17) as $T_m = \begin{pmatrix}T_1^{(2)}\\T_2^{(2)}\end{pmatrix}$. Hence, Eq. (17) becomes

$$\begin{pmatrix}E_t^{(2)+}\\0\end{pmatrix} = \begin{pmatrix}D_{11}^{(2)}E_0^{(2)+} + D_{12}^{(2)}E_0^{(2)-} + T_1^{(2)}\\D_{21}^{(2)}E_0^{(2)+} + D_{22}^{(2)}E_0^{(2)-} + T_2^{(2)}\end{pmatrix} \tag{19}$$

which gives the reflected and the transmitted SH field, respectively,

$$E_0^{(2)-}(2\omega) = -\frac{D_{21}^{(2)}E_0^{(2)+} + T_2^{(2)}}{D_{22}^{(2)}} \tag{20}$$

$$E_t^{(2)+}(2\omega) = \left(\frac{\det D^{(2)}}{D_{22}^{(2)}}\right)E_0^{(2)+} - \frac{D_{12}^{(2)}T_2^{(2)}}{D_{22}^{(2)}} + T_1^{(2)} \tag{21}$$

where $E_0^{(2)+}(2\omega)$ is the input second harmonic (seed) field. It is important to realize that, while the linear reflectivity and transmitivity $r^{(1)}$ and $t^{(1)}$ depend on ω they do not depend on the spectral content of the pump pulse. However, the nonlinear reflected $E_0^{(2)-}(2\omega)$ and transmitted $E_t^{(2)+}(2\omega)$ fields can depend on the spectral content of the pump pulse through $\Omega_0^{+}(\omega) = \Omega_0^{+}\exp[-\left(\frac{\omega-\omega_L}{\sigma_L}\right)^2]$.

To obtain the transmission $T^{(2)} = |t_2|^2$ and reflection $R^{(2)} = |r_2|^2$ spectra for SH electric fields, we divide the fields by the $\Omega_0^{+}(\omega) = \Omega_0^{+}$ amplitude of the pump field, i.e., $r_2 = \frac{E_0^{(2)-}}{\Omega_0^{+}}$ and $t_2 = \frac{E_t^{(2)+}}{\Omega_0^{+}}$. The reflected (superscript '−') and transmitted (superscript '+') fields in time domain are obtained by Fourier transform, $E_j^{(2)\pm}(z,t) = \mathcal{F}\{E_j^{(2)\pm}(z,\omega')\}$ and $\Omega_j^{(1)\pm}(z,t) = \mathcal{F}\{\Omega_j^{(1)\pm}(z,\omega)\}$.

3 Superconductor with temperature dependence

Now we apply two-fluid model to describe electromagnetic propagation in the superconducting layer at nonzero temperature [38, 39]. The electrical conductivity of a superconductor is

$$\sigma = \sigma_n + \sigma_s \tag{22}$$

where σ_n is conductivity of the unpaired normal electron with density of n_n, and σ_s is conductivity of paired superelectrons with density of n_s. The total electron number density is

$$n = n_n + n_s$$

The frequency-dependent conductivity at nonzero frequency is given in [41]

$$\sigma(\omega) = \frac{n\tau e^2}{m}\left[\frac{f_n}{1+(\omega\tau)^2} + i\left(\frac{f_n\omega\tau}{1+(\omega\tau)^2} + \frac{f_s}{\omega\tau}\right)\right] \tag{23}$$

where $f_n = \frac{n_n}{n}$ and $f_s = \frac{n_s}{n}$ are fluid fractions and τ is electron mean relaxation time, m and e are mass and charge of electron, respectively.

For excitations involving fields with higher frequencies that may exceed the superconducting bandgap $2\Delta(T)$ which depends on temperature T, we must introduce the notch functions [40]

$$f_\pm = \frac{1}{e^{\pm u}+1},\ u = \frac{\omega - 2\Delta}{k_BT},\ \Delta(T) = \Delta_0(1-x^3)^4 \tag{24}$$

into the conductivity

$$\sigma(\omega, T) = f_- \sigma^<(\omega) + f_+ \sigma^>(\omega) \tag{25}$$

where the conductivity for $\omega < 2\Delta$ is rewritten as

$$\sigma^<(\omega) = (1 - x^4) i \frac{ne^2}{m\omega} + x^4 \left(\frac{\sigma_{tot}}{1 - i\omega\tau} \right) \tag{26}$$

where $\frac{n_n(T)}{n} = x^4$, while the conductivity above the bandgap is essentially normal conductor

$$\sigma^>(\omega) = \frac{\sigma_{tot}}{1 - i\omega\tau} \tag{27}$$

where $\sigma_{tot} = \frac{ne^2\tau}{m}$ and $n = \frac{m}{\mu_0 e^2 \lambda_d^2(0)}$ with $\lambda_d(0)$ as the penetration depth at absolute zero. Since $\frac{1}{\lambda_d^2(T)} = \frac{n_s(T)\mu_0 e^2}{m}$ we have $\frac{\lambda_d^2(0)}{\lambda_d^2(T)} = \frac{n_s(T)}{n} = 1 - x^4 < 1$.

The dielectric function of superconductor is related to $\sigma(\omega, T)$ by

$$\varepsilon_s(\omega) = \varepsilon_b + i \frac{\sigma(\omega)}{\varepsilon_0 \omega} \tag{28}$$

The frequency ω_f where Re ε_s flips from negative to positive can be estimated from

$$\frac{ne^2\tau^2}{\varepsilon_0 m} \left[f_- \left(1 - \frac{x^4}{1 + (\omega_f\tau)^2} \right) + f_+ \frac{(\omega_f\tau)^2}{1 + (\omega_f\tau)^2} \right] = (\omega_f\tau)^2 \tag{29}$$

We also include dispersive magnetic material as one of the layers, realized for example through interaction between SRR and magnetic field of the incident beam [42].

$$\mu_j(\omega) = 1 - \frac{F}{\omega^2 + \omega_{mj}^2 + i\omega\Gamma_j} \tag{30}$$

where F is fraction factor of SRR in the photonic crystal, Γ_j is the dissipation factor and ω_{mj} is the resonant frequency of SRR.

4 Results and discussion

The results in Fig. 2. are obtained using the following parameters without second harmonic seed, $E_0^{(2)+}$. For the structure, $d = 10$ μm, $d_1 = 0.5$ d, $N = 10$. For superconductor $\varepsilon_2(\omega)$ (in medium 2): $\varepsilon_b = 15, \lambda_d = 0.2$ d, $\tau = 10^{-13}$ s, $T_c = 300$ K, $\hbar\Delta_0 = 0.01$ eV. For magnetic material $\mu_2(\omega)$ (in medium 2): $\omega_{m1} = 2\Delta_0, \Gamma_1 = 2 \times 10^{12}\,\mathrm{s}^{-1}$, $F_1 = 0.55$. The permeability and dielectric in layer 1 are constant: $\varepsilon_1 = 3, \mu_1 = 1$. The nonlinearity parameters of strontium barium niobate (SBN) is $\chi_1^{(2)} = 27.2$ pm/V and for the incident laser pulse $\omega_L = 2\Delta_0, \sigma_L = \Delta_0$.

Using the above parameters for superconductor, the frequency ω_f where ε_s in Eq. 29 is zero turns out to be in the far infrared region $\sim 10^{13}\,\mathrm{s}^{-1}$, which is close to the superconducting gap, $2\Delta_0 \simeq 3 \times 10^{13}\,\mathrm{s}^{-1}$. The magnetic resonance ω_{m1} lies below ω_f in Fig. 2a. This creates a narrow region of negative refractive index for medium 2 but it has little effect on the output of broadband pulse since it covers only a narrow resonance region of the magnetic permeability. Since medium 1 has constant ε_1 and μ_1 it is non-absorptive and non-dispersive.

Several interesting features are found for the pulse propagation in the nonlinear periodic medium. The presence of multiple passbands in the frequency domain (reflection and transmission spectra of Fig. 2a) translates into modulated pulse with short sub-pulses in the time domain (see Fig. 2b). Since the SH pulse exists only when the pump pulse is present, the points where the output pump intensity is zero give no SH signal at output (see Figs. 2 and 3), but the reverse may not be true. The number of subpulses increases with the spectral bandwidth of the input pulse (Fig. 2c), as it covers a larger number of passbands. This could be a new mechanism for generating a modulated or broken pulse containing short sub-pulses by breaking up the dispersion into photonic bands. It is also observed that reflected SH spectra are higher than the transmitted SH spectra by one order of magnitude. This is because the frequency region falls around the resonance frequencies of the magnetic and superconducting layers.

We observe from Figs. 2b and c the time delayed effect of the output pump and SH pulses. The slow light effect is more significant on the transmitted pulse propagating in the forward direction. It is not uniquely due to the nonlinear effect, but a result of multiple reflection and strong dispersion around the resonance region. Also, the reflected pump and SH pulses are stronger than transmitted pulses because strong reflection usually occurs around the absorption regions of the materials.

The temperature dependence in the reflection and transmission spectra is not prominent except close to the zero point frequency ω_f region which shows stronger temperature dependence due to the high sensitivity of the superconducting dielectric function in this region. At around and below ω_f, there is essentially no transmitted SH signal except at low temperature.

When medium 1 is magnetic and medium 2 is superconductor, in Fig. 3, the temperature dependence of the SH spectra can be seen more clearly. The reflected SH pulse shows interesting feature, a long pulse containing many sub-pulses, almost periodically spaced, extending over larger times. The slow light effect becomes more significant. This could be due to the strong dispersion and resonance in both medium 1 and medium 2, not only in medium 2 as in case of Fig. 2. This causes the group velocity delay, not just in medium 2 but also in medium 1.

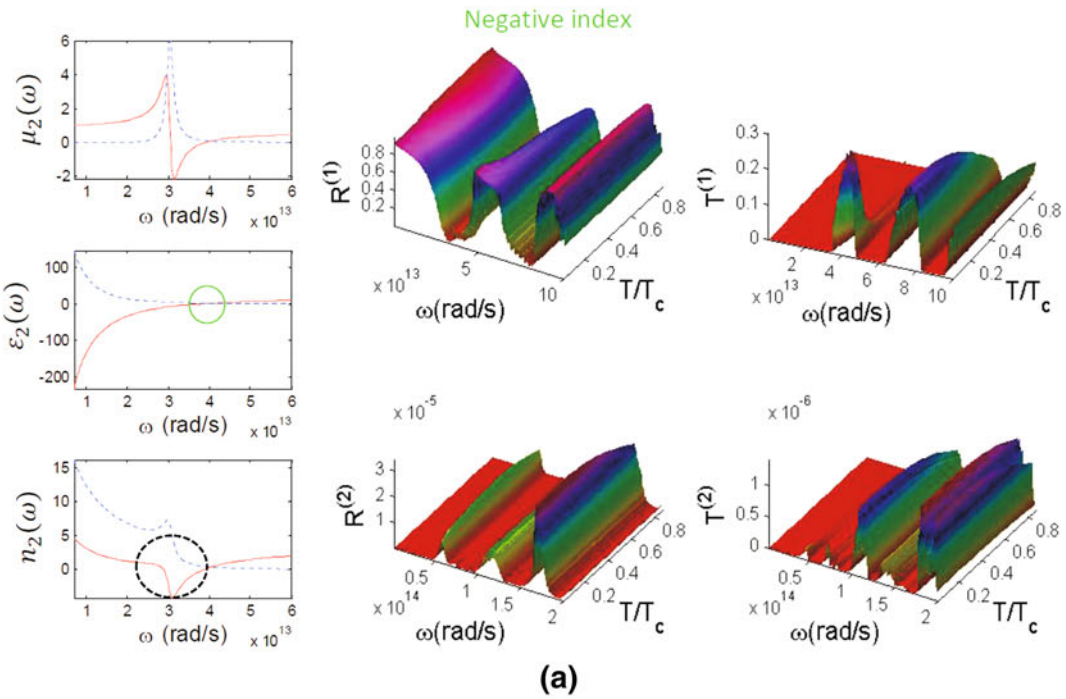
Negative index
$\mu_2(\omega)$
$\varepsilon_2(\omega)$
$n_2(\omega)$
ω (rad/s)
x 10^13
$R^{(1)}$
$T^{(1)}$
$R^{(2)}$
$T^{(2)}$
x 10^-5
x 10^-6
x 10^13
x 10^14
ω(rad/s)
T/T_c
(a)

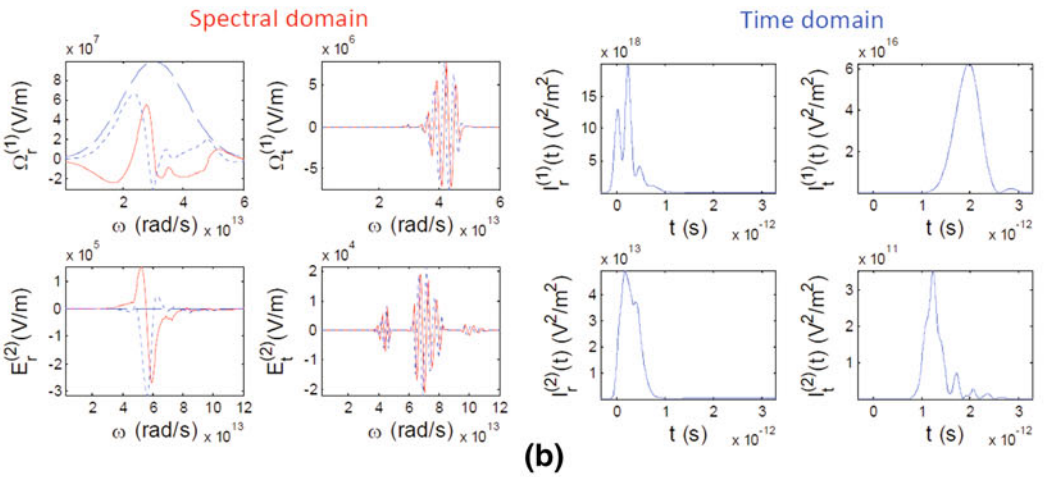
Spectral domain
Time domain
$\Omega_r^{(1)}$(V/m)
$\Omega_t^{(1)}$(V/m)
$E_r^{(2)}$(V/m)
$E_t^{(2)}$(V/m)
$I_r^{(1)}(t)$ (V²/m²)
$I_t^{(1)}(t)$ (V²/m²)
$I_r^{(2)}(t)$ (V²/m²)
$I_t^{(2)}(t)$ (V²/m²)
ω (rad/s) x 10^13
t (s) x 10^-12
(b)

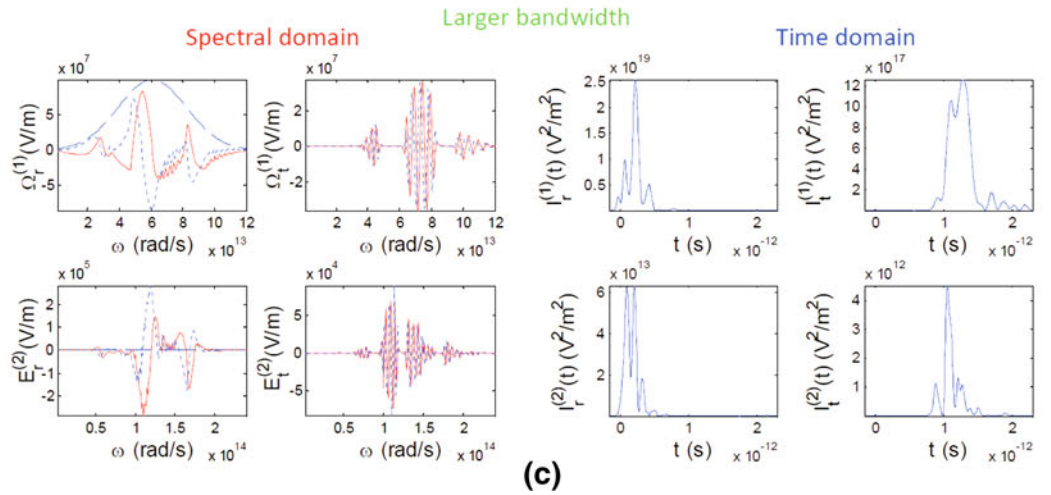
Larger bandwidth
Spectral domain
Time domain
$\Omega_r^{(1)}$(V/m)
$\Omega_t^{(1)}$(V/m)
$E_r^{(2)}$(V/m)
$E_t^{(2)}$(V/m)
$I_r^{(1)}(t)$ (V²/m²)
$I_t^{(1)}(t)$ (V²/m²)
$I_r^{(2)}(t)$ (V²/m²)
$I_t^{(2)}(t)$ (V²/m²)
ω (rad/s) x 10^13
x 10^14
t (s) x 10^-12
(c)

◀ **Fig. 2** **a** Real part (*solid line*) and imaginary part (*dotted line*) of μ, ϵ and n versus frequency. Transmission and reflection spectra versus normalized temperature T/T_c for the resonance with negative refractive index. **b** Output (electric field $\Omega_{r,t}, E^{(2)}_{r,t}$ and electric field squared $I^{(1)}_{r,t} = |\Omega_{r,t}|^2, I^{(2)}_{r,t} = |E^{(2)}_{r,t}|^2$) of reflected and transmitted pulses in time and frequency domains. Real part of field (*solid line*) and imaginary part (*dotted line*). **c** Output reflected and transmitted pulses for input pulse with larger bandwidth. The pulses are for temperature $T = 0.09\ T_c$. *Solid circle* shows ω_f while the *dashed circle* highlights the negative refractive index region. The input field is $\Omega_0^+ = 10^8$ V/m

We note that the modulated/distorted output pump pulse shown in Figs. 2 and 3 is entirely due to linear process of multiple scattering in the multilayers while the SH pulse produced is due to nonlinear (second harmonic) process. Significant distortion in the fundamental input pump pulse Ω_0^+ (with Gaussian spectrum) can be seen in Fig. 2 by comparing it with the fundamental output pulses $\Omega_r^{(1)}$ and $\Omega_t^{(1)}$. We find that the peak value of the output pulse is smaller than the peak of the input pulse, but the effective pulse duration is slightly larger. It is the result of absorption and multiple scattering (reflections and transmissions), but nonlinearity has no effect here. Thus, the pulse reshaping is entirely due to linear scattering process. Now, if we compare the second harmonic fields $E_r^{(2)}$, $E_t^{(2)}$ with the fundamental fields Ω_r, Ω_t in the spectral domain, we see that both are significantly different. They are different because the SH fields are due to the nonlinear process, in addition to the linear process of multiple scattering.

We clarify that the SH output should not be considered as pulses, as it simply appears to have been a fraction of

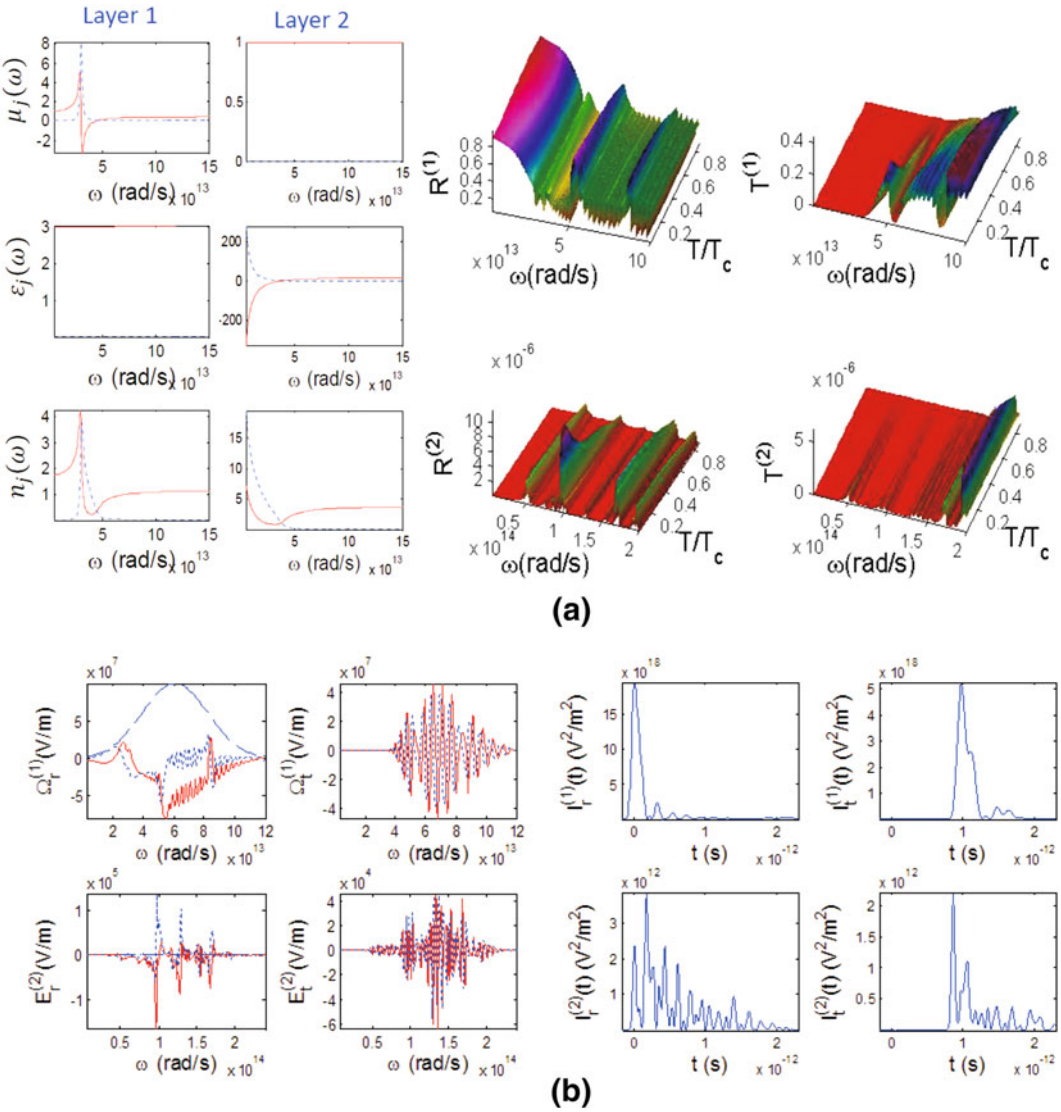

Fig. 3 Medium 1 is magnetic and medium 2 is superconducting showing **a** temperature-dependent spectra, **b** pulses in spectral and time domains

energy from the pump pulse that has been produced by nonlinear frequency conversion and strongly modulated by linear process of multiple scattering into sub-pulses. The multiple peaks of the field amplitude in the spectral domain does not guarantee that there are also similar peaks in the time domain due to the fact that the phase, i.e., the imaginary part, also plays a role when Fourier transforming to the time domain. The output pulse may seem chaotic but there is no statistical nor random process involved. Instead, several underlying physical processes are molding/modulating/shaping the resulting pulse. The output pulse may be useful that it contains some information about the mixture of optical processes; namely multiple scattering, propagation and second harmonic generation in the nonlinear photonic crystal. The results help to better understand the underlying optical processes such as dispersion, phase matching and slow light that lead to intensity modulation or breakup of the pump pulse and production of a strongly modulated SH pulse. Thus, this work forms a foundation for future works aimed at optimizing pulse modulation for applications such as in spectroscopy.

5 Conclusions

We have shown that photonic crystal with superconducting layer and second-order nonlinearity can be used to produce mid- or far-infrared (MIR–FIR) pulse using a nonlinear material through second harmonic generation process. An input (Gaussian) pump pulse is dramatically distorted and becomes shorter due to the strong dispersion and absorption around the resonant region of the magnetic material and the superconducting bandgap, as well as the multiple scattering. The nonlinear photonic crystal with superconducting and magnetic materials provides an alternative way to specialized crystals [43] to convert IR pulse to higher harmonics/frequencies and simultaneously reshaping the IR pulse through multiple scattering and nonlinear process at around the resonances of materials. The input IR pulse may be supplied from free electron laser [44]. We emphasize that there is no amplification nor lasing process involved in the nonlinear photonic crystal due to the small conversion efficiency, the absence of lasing cavity and no continuous energy pumping. The main mechanism here is nonlinear frequency conversion that produces second harmonic pulse in the IR wavelengths. At low temperature, the superconducting layer provides higher SHG conversion efficiency. Thus, the magnetic and superconducting nonlinear photonic crystal provides a new mechanism for reshaping and converting short pulse by combining resonant multiple scattering and nonlinear optical process for photonic spectral engineering.

Acknowledgments This work is supported by the Ministry of Higher Education (MOHE)/University of Malaya HIR Grant No. A-000004-50001 and the MOHE ERGS Grant No. ER014-2011A.

References

1. G. Guida, de A. Lustrac, A. Priou, An Introduction to photonic band gap (PBG) materials. Prog. Electromagn. Res. **41**, 1–20 (2003)
2. Soukoulis C.M. *Photonic band gap materials* (Kluwer, Dordrecht, 1996)
3. Quimby R.S. *Photonics and lasers: an introduction* (John Wiley and Sons, New York, 2006)
4. C.G. Ribbing, H. Hogstrom, A. Rung, Studies of polaritonic gaps in photonic crystals. Appl. Opt. **45**, 1575–1582 (2006)
5. P.A. Franken, A.E. Hill, C.W. Peters, G. Weinreich, Generation of optical harmonics. Phys. Rev. Lett. **7**, 118–119 (1961)
6. M. Scalora, M.J. Bloemer, A.S. Manka, J.P. Downling, C.M. Bowden, R. Viswanathan, J.W. Haus, Pulsed second-harmonic generation in nonlinear, one-dimensional, periodic structures. Phys. Rev. A **56**, 3166–3174 (1997)
7. J. Rudnick, E.A. Stern, Second-harmonic radiation from metal surfaces. Phys. Rev. B **4**, 4274–4290 (1971)
8. S.C. Lim, Magnetic second-harmonic generation of an antiferromagnetic film. J. Opt. Soc. Am. B **19**, 1401–1410 (2002)
9. S. Zhou, H. Li, S. Fu, X. Wang, Second harmonic generation from an antiferromagnetic film in one-dimensional photonic crystals. Phys. Rev. B **80**, 205409 (2009)
10. G. D'Aguanno, M. Centini, M. Scalora, C. Sibilia, Y. Dumeige, P. Vidakovic, J.A. Levenson, M.J. Blomer, C.M. Bowden, J.W. Haus, M. Bertolotti, Photonic band edge effects in finite structures and applications to $\chi^{(2)}$ interactions. Phys. Rev. E **64**, 016609 (2001)
11. J. Leuthold, C. Koos, W. Freude, Nonlinear silicon photonics. Nat. Photonics **4**, 535–544 (2010)
12. G. Khanarian, R.A. Norwood, D. Haas, B. Feuer, D. Karim, Phase-matched second-harmonic generation in a polymer waveguide. Appl. Phys. Lett. **57**, 977–979 (1990)
13. M. Yamada, N. Nada, M. Saitoh, K. Watanabe, First-order quasi-phase matched $LiNbO_3$ waveguide periodically poled by applying an external field for efficient blue second-harmonic generation. Appl. Phys. Lett. **62**, 435–436 (1993)
14. H. Cao, D.B. Hall, J.M. Torkelson, C.Q. Cao, Large enhancement of second harmonic generation in polymer films by microcavities. Appl. Phys. Lett. **76**, 538–540 (2000)
15. B. Shi, Z.M. Jiang, X. Wang, Defective photonic crystals with greatly enhanced second-harmonic generation. Opt. Lett. **26**, 1194–1196 (2001)
16. D. Faccio, F. Bragheri, Localization of light and second-order nonlinearity enhancement in weakly disordered one-dimensional photonic crystals. Phys. Rev. E **71**, 057602 (2005)
17. R. Iliew, C. Etrich, T. Perstsch, F. Lederer, Slow-light enhanced collinear second-harmonic generation in two-dimensional photonic crystals. Phys. Rev. B **77**, 115124 (2008)
18. R. Iliew, C. Etrich, T. Perstsch, F. Lederer, Y.S. Kivshar, Huge enhancement of backward second-harmonic generation with slow light in photonic crystals. Phys. Rev. A **81**, 023820 (2010)
19. Y. Kong, X. Chen, T. Zhu, Intensity modulation on polarization coupling and frequency conversion in periodically poled lithium niobate. Appl. Phys. B **102**, 101–107 (2011)
20. M.L. Ren, Z.Y. Li, Giant enhancement of second harmonic generation in nonlinear photonic crystals with distributed Bragg reflector mirrors. Opt. Express **17**, 14502–14510 (2009)

21. J. Bardeen, Two-fluid model of superconductivity. Phys. Rev. Lett. **1**, 399–400 (1958)
22. D.S. Linden, T.P. Orlando, W.G. Lyons, Modified two-fluid model for superconductor surface impedance calculation. IEEE Trans. Appl. Supercond. **4**, 136–142 (1994)
23. C.J. Wu, C.L. Liu, T.J. Yang, Investigation of photonic band structure in a one-dimensional superconducting photonic crystal. J. Opt. Soc. Am. B **26**, 2089–2094 (2011)
24. C.J. Wu, Y.L. Chen, Microwave properties of a high-temperature superconductor and ferromagnetic bilayer structure. Prog. Electromagn. Res. **111**, 433–445 (2011)
25. Z. Huang, C. Tu, S. Zhang, Y. Li, F. Lu, Y. Fan, E. Li, Femtosecond second-harmonic generation in periodically poled lithium niobate waveguides written by femtosecond laser pulses. Opt. Lett. **35**, 877–879 (2010)
26. K. Kuroda, Y. Toga, T. Satoh, T. Shimura, S. Ashihara, Y. Takahashi, M. Yoshimura, Y. Mori, T. Sasaki, Generation of mid/far-infrared ultrashort pulses in organic crystals. J. Phys. Conf. Ser. **206**, 012104 (2010)
27. J.B. Pendry, A.J. Holden, D.J. Robbins, W.J Stewart, Magnetsim from conductors and enhanced nonlinear phenomena. Trans. Microw. Theory Tech. **47**, 2075–2084 (1999)
28. J.B. Pendry, A.J. Holden, W.J. Stewart, I. Youngs, Extremely low frequency plasmons in metalic mesostructures. Phys. Rev. Lett. **76**, 4773–4776 (1996)
29. M.W. Klein, C. Enkrich, M. Wegener, S. Linden, Second-harmonic generation from magnetic metamaterials. Science **313**, 502–504 (2006)
30. A. Rose, D. Huang, D.R. Smith, Controlling the second harmonic in a phase-matched negative-index metamaterial. Phys. Rev. Lett **107**, 063902 (2011)
31. V.G. Veselago, The electrodynamics of substances with simultaneously negative values of ε and μ. Sov. Phys. Usp. **10**, 509–514 (1968)
32. W.J. Padilla, D.N. Basov, D.R. Smith, Negative refractive index metamaterials. Mater. today **9**, 28–35 (2006)
33. P. Yeh, A. Yariv, C.S. Hong, Electromagnetic propagation in periodic stratified media. I. General theory. J. Opt. Soc. Am. **67**, 423–438 (1977)
34. D.S. Bethune, Optical harmonic generation and mixing in multilayer media: analysis using optical transfer matrix techniques. J. Opt. Soc. Am. B **6**, 910–916 (1986)
35. J.J. Li, Z.Y. Li, D.Z. Zhang, Second harmonic generation in one-dimensional nonlinear photonic crystals solved by the transfer matrix method. Phys. Rev E **75**, 056606 (2007)
36. D. Faccio, F. Bragheri, M. Cherchi, Optical Bloch-mode-induced quasi phase matching of quadratic interactions in one-dimensional photonic crystals. J. Opt. Soc. Am. B **21**, 296–301 (2004)
37. M. Born, E. Wolf, Principles of optics, 7th edn. (Pergamon Press, New York, 1999)
38. C.H.R. Ooi, T.C. Au Yeung, C.H. Kam, T.K. Lim, Photonic band gap in a superconductor-dielectric superlattice. Phys. Rev. B **61**, 5920–5923 (2000)
39. C.H.R. Ooi, T.C. Au Yeung, Polariton gap in a superconductor–dielectric superlattice. Phys. Lett. A **259**, 413–419 (1999)
40. H. Rauh, Y.A. Genenko, J. Phys. Condens. Matter **20**, 145203 (2008)
41. C.H.R. Ooi, C.H. Kam, Echo and ringing of optical pulse in finite photonic crystal with superconductor and dispersive dielectric. J. Opt. Soc. Am. B **27**, 458–463 (2010)
42. D.R. Smith, W.J. Padilla, D.C. Vier, S.C. Nermat-Nasser, S. Schultz, Composite medium with simultaneously negative permeability and permittivity. Phys. Rev. Lett. **84**, 4184–4187 (2000)
43. N.A. van Dantzig, P.C.M. Planken, H.J. Bakker, Far-infrared second-harmonic generation and pulse characterization with the organic salt DAST, Opt. Lett. **23**, 466–468 (1998)
44. G.M.H. Knippels, R.F.X.A.M. Mols, A.F.G. van der Meer, D. Oepts, P.W. van Amersfoort, Intense far-infrared free-electron laser pulses with a length of six optical cycles. Phys. Rev. Lett. **75**, 1755–1758 (1995)